PSNR Enhancement in Image Streaming over Cognitive Radio Sensor Networks

Mahdi Bahaghighat and Seyed Ahmad Motamedi

Several studies have focused on multimedia transmission over wireless sensor networks (WSNs). In this paper, we propose a comprehensive and robust model to transmit images over cognitive radio WSNs (CRWSNs). We estimate the spectrum sensing frequency and evaluate its impact on the peak signal-to-noise ratio (PSNR). To enhance the PSNR, we attempt to maximize the number of pixels delivered to the receiver. To increase the probability of successful image transmission within the maximum allowed time, we minimize the average number of packets remaining in the send buffer. We use both single- and multi-channel transmissions by focusing on critical transmission events, namely hand-off (HO), No-HO, and timeout events. We deploy our advanced updating method, the dynamic parameter updating procedure, to guarantee the dynamic adaptation of model parameters to the events. In addition, we introduce our ranking method, named minimum remaining packet best channel selection, to enable us to rank and select the best channel to improve the system performance. Finally, we show the capability of our proposed image scrambling and filtering approach to achieve noticeable PSNR improvement.

Keywords: Cognitive radio, Image filtering, Multimedia transmission, PSNR, Spectrum sensing, Wireless Sensor Networks.

Manuscript received Dec. 2, 2016; revised May 26, 2017; accepted July 24, 2017.
Seyed Ahmad Motamedi (corresponding author, motamedi@aut.ac.ir) and Mahdi Bahaghighat (m.bahaghighat@aut.ac.ir) are with the Wireless Sensor Laboratory, Electrical Engineering Department, Amirkabir University of Technology, Tehran, Iran.

I. Introduction

In recent decade, a lot of researches have been conducted on wireless sensor networks (WSNs). Currently, this concept covers different aspects of communication network technologies and applications. Similar to other wireless networks, multimedia transmission over WSNs (WMSNs) is a challenging issue [1]. Wireless multimedia applications require significant bandwidth and often have to satisfy relatively tight delay constraints. In addition, delay-sensitive data transmission, such as image transmission, conflicts with the limited available WSN resources. Although much work has been done in the field of WMSNs, to date, this problem has remained unsolved [2]. The main obstacle that hinders the development of WMSNs is the band-limited nature of traditional WSNs.

Generally, radio spectrum is a scarce resource. The limited availability of bandwidth is considered one of the major bottlenecks that hinder the development of high-quality multimedia wireless services [3]. The concept of the cognitive radio sensor network (CRSN or CRWSN) was first introduced by [4]. However, up to the present there have been few reported studies on image transmission over light and low end devices in CRSNs. Multimedia and delay-sensitive data applications in CRSNs require efficient real-time communication and dynamic spectrum access (DSA) capabilities [5]. Compared with traditional WSNs, intelligent DSA in CRSNs not only improves spectral utilization, but also enhances the quality of service (QoS) in multimedia transmission systems. Delay-sensitive and multimedia communication in CRSNs was introduced by [5], but their model was customized for only 500 kV substations. A similar idea was also proposed by [6].

On the other hand, optimal spectrum sensing is a key enabling technology for cognitive radio networks. The

main objective of spectrum sensing is to provide more spectrum-access opportunities to cognitive radio users without interfering with the operations of licensed network users [7]. Spectrum sensing has the potential to significantly impact the QoS [8] in both primary and secondary networks. A large inter-time spacing between two successive spectrum sensing (SS) runs may lead to collision, and consequently retransmission, while a small inter-time spacing can increase the overhead of systems in terms of time and power consumption. Realizing the lifetime maximization of a node is an important challenge in WSNs, and is directly related to power consumption [9]. The use of orthogonal frequency-division multiplexing (OFDM) based traffic allocation in the subchannels of spectrum pools is an appropriate method for increasing the system reliability [10], but there have been few reported works that focus on multichannel image transmission over CRSNs.

Reference [11] demonstrates a new model that exploits the impact of an SS frequency and packet-loading scheme for multimedia transmission over cognitive radio networks. Although their approach was the first work that derived the benefits from the SS frequency, their model suffers from a nonadaptive structure during multimedia transmission, high complexity, and large processing time, which is not suitable for resource-limited sensor nodes in WSNs.

In this paper, we model an effective approach to achieving image transmission over CRSNs, focusing on the image quality at the receiver. We developed an adaptive structure model based on SS frequency optimization. In our model, we focus on optimizing the SS frequency in order to minimize the number of packets remaining in the send buffer. The parameters of our model are dynamically adapted to channel situations, and our updating process, called the dynamic parameter updating procedure (DPUP) is applied depending on whether hand-off (HO) events occur or not. In addition, we apply our proposed channel-ranking procedure, minimum remaining packet best channel selection (MRBC) to increase the probability of successful transmission of the image within the maximum tolerable delay time. In order to improve the performance of the transmission system, we develop our work according to multichannel packet scheduling, and then we incorporate some image processing based approaches to increase PSNR as much as possible; so, we end up our proposed PSNR enhancement method by scrambling the image in the transmitter and applying average filtering enhancement in the receiver (MC-SAFE), which significantly affects the final PSNR.

II. Proposed Model

In this section, we present our proposed model for image transmission over CRSNs.

1. Primary User Activity Model

In CRNs, the primary user activity significantly impacts the network performance, and it is difficult to obtain a good estimate of this activity in SS. According to most related works, we assume that primary user (PU) activity can be modeled as exponentially distributed inter-arrival times. In this applicable model, the traffic regime of the PUs can be considered as a two-state birth-death process (BDP), with a death rate of α and a birth rate of β. An ON (Busy) state represents the period used by PUs, while an OFF (Idle) state represents the unused period [12], [13]. Based on the assumption of independent arrival of the PUs, each transition follows the Poisson arrival process. Thus, the lengths of ON and OFF periods are exponentially distributed, and PU activity can be modeled as exponentially distributed inter-arrival times.

2. Secondary User Activity Model

The secondary user (SU) activity in CRSNs can be restricted by the PU's arrival. When a PU reoccupies the channel that would be "Idle" in the last SU's sensing period, the SU must vacate the current channel to prevent additional degradation of the QoS in the PU's network. In this case, the SU should try to switch to an alternate channel J in the available channel list (J = 1, 2, 3, . . . , S0; where S0 is the number of available channels in the spectrum pool).

As mentioned before, the PU arrival process in an arbitrary channel i is modeled as a Poisson process with the parameter λ_i (that is, the arrival rate); therefore, the PU inter-arrival time τ_i will be an exponential distribution, with the mean arrival time given as $\mu_i = 1/\lambda_i$ [2], [5].

3. Adaptive Image Transmission Through Single Channel

For image transmission, it is assumed that the image data stream can be fitted into N packets. Therefore, N indicates the total number of picture packets that are available in the send buffer before transmission. In the beginning phase of the image transmission, an active SU makes its decision among S available licensed channels in the spectrum pool (our new channel selection process will be explained at the end of this section). After the selection of an available idle channel, the SU turns on its RF link and begins to transmit the packet streams over the air medium.

https://doi.org/10.4218/etrij.17.0116.0887

Generally, wireless multimedia transmission systems require significant bandwidth and often have to satisfy relatively tight delay constraints. In related works [3], [11], $D_{\max}$ is defined as the maximum tolerable time in which an image data stream, including N packets, should be sent by the transmitter. From this definition, the reception of any packet after $D_{\max}$ indicates that some packets were lost during transmission, and the PSNR of the image at the receiver may be highly degraded.

Here, we define the channel capacity R_i as the total number of packets that can be transmitted during $D_{\max}$. It has been reported in some previous works [2], [3] that some major metrics in SS models, such as the probability of correct spectrum detection (P_{CD}), the probability of false alarm (P_{FA}), and the probability of miss detection (P_{MD}), can play key roles in the performance of CRNs. In the same way, as reported by [11], we prefer to evaluate the impacts of P_{FA}; therefore, we assume that $P_{\mathrm{CD}} = 1$ and $P_{\mathrm{MD}} = 0$.

As previously mentioned, the impacts of the SS frequency and packet-loading scheme on multimedia transmission over cognitive radio networks have been investigated by [11]. They introduced their new and creative model to perform the SS procedure using a periodic pattern. Further, they defined parameter f as the number of packets that are ready to be sent before running the next SS. Inter-sensing time $t_i, t_i = f_i t_{\mathrm{p}} + T_{\mathrm{Sensing}}$, $t_{\mathrm{p}} = D_{\max}/R_i$, represents the actual time between two successive SS iterations in the channel "i". Using this notation, f_i is the number of packets that should be transmitted over channel "i" before running the spectrum sensing once more, and t_{p}, T_{Sensing} are the packet time and sensing time duration, respectively. Here, increasing "f" means that the number of SS iterations decreases, and as a result, the SS time overhead will experience a noticeable reduction. This reduced time overhead may increase the probability of achieving successful image transmission within the time range [0, $D_{\max}$].

On the other side, by increasing f without any constraint, the probability of collision between PUs and SU in the re-occupied channel will significantly increase. This phenomenon requires intelligent trade-offs between the collision probability and time overhead. This tradeoff can be handled by optimizing parameter "f" according to an appropriate cost function. In (1):

$$\begin{aligned} N_{\mathrm{RP}} &= \Delta N = N - N_i, \\ N_i &= X_i f_i, \end{aligned} \tag{1}$$

where N_{RP} is defined as the number of packets remaining in the send buffer after the X_ith round of continuous transmission of f_i packets in the channel "i" [11]. At this time, the SS shows that due to the new arrival of some PUs, the channel "i" is no longer available; therefore, the sensor node should switch to a new idle channel (such as j) to fulfil the transmission task.

Based on the PU's activity model mentioned earlier, the probability $P\{X_i \geq x\}$ can be written as follows [11]:

$$\begin{cases} P\{X_i \geq 0\} = 1, P\{X_i \geq 1\} = (1 - P_{\mathrm{FA}})e^{-\lambda_i t_i} \\ P\{X_i \geq 2\} = 1(1 - P_{\mathrm{FA}})^2 e^{-\lambda_i 2t_i} \\ . \\ . \\ . \\ P\{X_i \geq K_i\} = (1 - P_{\mathrm{FA}})^{K_i} e^{-\lambda_i K_i t_i} \end{cases} \tag{2}$$

where $K_i = [N/f_i]$. In (3), the outcome of the last equation is presented:

$$\begin{cases} P\{X_i = 0\} = 1, (1 - P_{\mathrm{FA}})e^{-\lambda_i t_i} \\ P\{X_i = 1\} = (1 - P_{\mathrm{FA}})e^{-\lambda_i t_i} - (1 - P_{\mathrm{FA}})^2 e^{-\lambda_i 2t_i} \\ P\{X_i = 2\} = (1 - P_{\mathrm{FA}})^2 e^{-\lambda_i 2t_i} - (1 - P_{\mathrm{FA}})^3 e^{-\lambda_i 3t_i} \\ . \\ . \\ . \\ P\{X_i = K_i\} = (1 - P_{\mathrm{FA}})^{K_i} e^{-\lambda_i K_i t_i}. \end{cases} \tag{3}$$

Now, we can estimate the mathematical expectation of the remaining packets in the sending buffer $E(N_{\mathrm{RP}})$ [11]:

$$\begin{aligned} E(N_{\mathrm{RP}}) &= \sum_{n=0}^{K_i} (N - nf_i) P\{X_i = n\} \\ &= N(1 - a^{K_i}) - f_i \frac{a - a^{K_i}}{1 - a} + f_i (K_i - 1) a^{K_i} \\ &= N - f_i \frac{a(1 - a^{K_i})}{1 - a}, a = (1 - P_{\mathrm{FA}})e^{-\lambda_i t_i}. \end{aligned} \tag{4}$$

Clearly, the limit of $E(N_{\mathrm{RP}})$ as λ_i approaches infinity will be equal to N:

$$\lim_{\lambda_i \to \infty} E(N_{\mathrm{RP}}) = N. \tag{5}$$

This implicitly indicates that if PU's channels are in the saturation state, there are always N packets in the transmission buffer waiting to be sent. Therefore, in this study, we consider the unsaturated channel condition to investigate the results of our model.

Similarly, in our work, $E(N_{\mathrm{RP}})$ is defined as the cost function, and according to (6), the target is to accurately estimate f_i* in order to minimize the cost of the system.

$$\begin{aligned} \min E(N^i{}_{\mathrm{RP}}) = \min g(f_i; \lambda_i, T_{\mathrm{Sensing}}, N, D_{\max}, P_{\mathrm{FA}}) \\ lb \leq f_i \leq ub. \end{aligned} \tag{6}$$

Without loss of generality and to enable a feasible solution, f_i should be between the upper and lower bounds, as indicated below:

$$\frac{NT_{\text{Sensing}}}{D_{\max}(1-\frac{N}{R_i})} \le f_i \le R_i. \quad (7)$$

To estimate f_i*, we extract the following results from the equation $d/df_i(E(N_{\text{RP}})) = 0$:

$$\begin{aligned} f^*{}_i &\approx \Delta f = f_+ - f_-, \\ f_+ &= \frac{1}{A}\sqrt{P_{\text{FA}} + T_{\text{Sensing}}\left(\frac{R_i A}{D_{\max}}\right) - \frac{CNP_{\text{FA}}B}{1-B}}, \\ f_- &= \frac{(P_{\text{FA}} + T_{\text{Sensing}}\left(\frac{R_i A}{D_{\max}}\right))}{A}, \\ A &= (1-P_{\text{FA}})\lambda_i \frac{D_{\max}}{R_i},\ B = e^{-\lambda_i \frac{D_{\max}}{R_i}N}. \end{aligned} \quad (8)$$

Figure 1 demonstrates the impact of the maximum tolerable delay, $D_{\max}$, and f_i on $E(N_{\text{RP}})$. As shown in the figure, $D_{\max}$ is increased from 0.1 s to 3 s in four independent scenarios. In the first scenario, $D_{\max}$ = 0.1 s, and the lowest f_i is selected as the optimum point, while the highest number of packets (more than 600 packets) remain in the send buffer, compared to less than 275 packets in the last scenario ($D_{\max}$ = 3) with the highest value of f_i, for the first round of transmission.

Reference [11] constructed a model based on the optimization of $E(N_{\text{RP}})$ at the beginning of transmission on the available channel "i," and before HO of the current channel to the alternate channel "j" due to the arrival of the PU. However, in our work, we consider the critical situation after each HO to update the parameters in our system based on the new channel access scenario. Consequently, we applied our proposed procedure with dynamic updating of important parameters (DPUP), as indicated by Procedure 1.

Figure 2 depicts our proposed system model and its dynamic updating approach depending on two different states: HO and no HO (NHO).

First, consider the condition where there is no need for an HO after a new SS. This implies that we have a

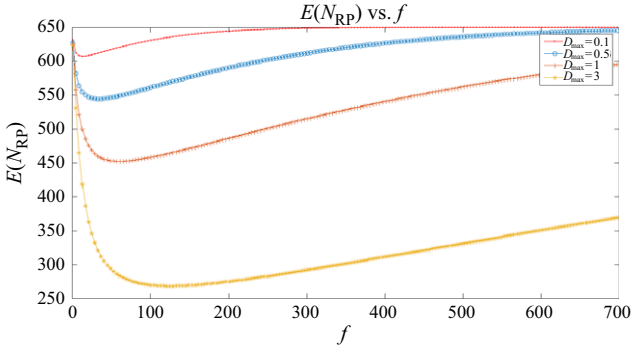

Fig. 1. Impact of maximum tolerable delay on mathematical expectation of remaining packets.

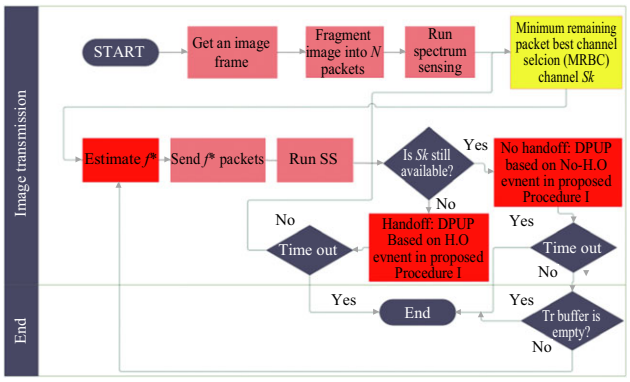

Fig. 2. Proposed Methods for Image Transmission over CRSN.

Procedure 1. Dynamic Parameters Updating Procedure (DPUP)

if Hand − off not occured

if $N^{(K+1)} > 0$ && $D_{\max}{}^{(K+1)} > 0$

Channel Condition:

$i \to j, i = CurrentChannel$ & $j = NextChannel$ & $i = j$

Maximum Tolerable Delay:

$D_{\max}{}^{(K)} \to D_{\max}{}^{(K+1)} = D_{\max}{}^{(K)} - (N^{(K)} - E^{(K)}(N_{\text{RP}})) \times t_i)$

$N^{(K+1)} = N^{(K)} - E^{(K)}(N_{\text{RP}})$

$f_i^{(K+1)}$: *estimated from* $\frac{d(E_i{}^{(K+1)}(N^{(K+1)}))}{dt} = 0$

End

else if Hand − off occured

if $N^{(K+1)} > 0$ && $D_{\max}{}^{(K+1)} > 0$

Channel Condition:

$i \to j, i = CurrentChannel$ & $j = NextChannel$ & $i \neq j$

Maximum Tolerable Delay:

$D_{\max}{}^{(K)} \to D_{\max}{}^{(K+1)} = D_{\max}{}^{(K)} - (N^{(K)} - E^{(K)}(N_{\text{RP}})) \times t_i)$

$N^{(K+1)} = N^{(K)}$

$f_j^{(K+1)}$: *estimated from* $\frac{d(E_j{}^{(K+1)}(N^{(K)}))}{dt} = 0$

End

End

successful transmission of "f" packets in round K; and both parameters $D_{\max}{}^{(K)}$ and $N^{(K)}$ should therefore be updated to extract $f_i^{(K+1)}$ from:

$$\frac{d(E_i{}^{(K+1)}(N^{(K+1)}))}{dt} = 0. \quad (9)$$

Second, in the situation where the HO is an obligation owing to the new arrival of PUs, it is interpreted as a collision event during the last transmission of $f_i^{(K)}$ packets; thus, about $f_i^{(K)}$ packets may be lost, and they should be retransmitted in the new channel j. Therefore, only $D_{\max}{}^{(K)}$

will be updated to $D_{\max}{}^{(K+1)}$, and $N^{(K+1)}$ will remain the same as $N^{(K)}$. In this case, we can obtain $f_j^{(K+1)}$ from (10):

$$\frac{d(E_j^{(K+1)}(N^{(K)}))}{dt} = 0. \tag{10}$$

In addition to updating parameters dynamically to best adapt to the $E(N_{\mathrm{RP}})$ based on channels and timing conditions, we add our proposed rule to select the optimized channel from the spectrum after running the SS. This task can be effectively carried out by selecting the best channel that minimizes $E_n^{(K)}(N_{\mathrm{RP}})$. We call this process MRBC, and it is formulated as shown:

$$\begin{aligned}
&j = Arg\min(E_n^{(K)}(N_{\mathrm{RP}})), \mathrm{All}\, n \in A \& n \neq i \\
&\min E_n^{(K)}(N_{\mathrm{RP}}) = g(f_n; \lambda_n, N^{(K+1)}, D^{(K+1)}{}_{\max}, T_{\mathrm{Sensing}}, P_{\mathrm{FA}}) \\
&A \subset S, n(A) \leq s, n(A) \neq 0, A = \{k \in S | \psi(k) = 1\} \\
&\psi(k) = \begin{cases} 0 \text{ if channel } k \text{ is Busy} \\ 1 \text{ if channel } k \text{ is Empty.} \end{cases}
\end{aligned} \tag{11}$$

4. Packet Loading Through Multichannel Communication (MCPL)

In this section, we extend our proposed approach to multichannel transmission. In this case, an active SU can stream an N-packet input image into all of the S available channels simultaneously; thus, the sending SU fragments N packets into S fragments: $\{N_1, N_2, \ldots, N_S\}$ such that N_j refers to the number of packets that should be sent through the channel "j." Therefore, it follows that:

$$N = \sum_{j=1}^{S} N_j. \tag{12}$$

As a direct extension of the single-channel case, the remaining packets of all channels can be defined as the summation of the remaining packets of each channel [11]:

$$\begin{aligned}
E(N_{\mathrm{RP}}) = \sum_{i=1}^{S} E(N_{\mathrm{RP},i}) = \sum_{i=1}^{S} N_i(1 - a^{K_i}) - f_i \frac{a - a^{K_i}}{1 - a} \\
+ f_i(K_i - 1)a^{K_i}.
\end{aligned} \tag{13}$$

Now, we focus on the minimum of the $E(N_{\mathrm{RP}})$ function in order to achieve the optimum solution of this new problem. By evaluating the equation, it is clear that $E(N_{\mathrm{RP}})$ is the function of $\{N_1, N_2, \ldots, N_S\}$ and $\{f_1, f_2, \ldots, f_S\}$ variables, and it depends on the following parameters: $\{T_S, P_{\mathrm{FA}}, R_i, \lambda_1, \lambda_2, \ldots, \lambda_S\}$; therefore, the optimization problem has 2S variables and can be formulated as shown below:

$$\begin{aligned}
&E(N_{\mathrm{RP}}) \triangleq F(x_1, x_2, \ldots, x_S, x_{S+1}, x_{S+2}, \ldots, x_{2S}; T_S, P_{\mathrm{FA}}, \\
&\lambda_1, \lambda_2, \ldots, \lambda_S\} \min F(x_1, x_2, \ldots, x_S, x_{S+1}, x_{S+2}, \ldots, x_{2S}; \\
&T_S, P_{\mathrm{FA}}, \lambda_1, \lambda_2, \ldots, \lambda_S\}\{x_1, x_2, \ldots, x_S\} = \{N_1, N_2, \ldots, \\
&N_S\}, \{x_{S+1}, \ldots, x_{2S}\} = \{f_1, f_2, \ldots, f_S\} \\
&x_{S+i} \leq R_i, \text{for } i = 1, 2, \ldots, S, \sum_{i=1}^{S} x_i = \sum_{i=1}^{S} N_i = N.
\end{aligned} \tag{14}$$

To reduce the high complexity of this problem, [11] assumed that all channels have an equal value of "f" ($\{f_1 = f_2 = , \ldots, = f_S = f\}$), and that the channel rates are the same for all channels ($\{R_1 = R_2 = , \ldots, = R_S = R\}$). Consequently, the optimization problem is converted to a packet-loading problem and SS frequency optimization based on just $(S + 1)$ variables $V_s = \{N_1, N_2, \ldots, N_S, f\}$:

$$\begin{aligned}
&\min E(N_{\mathrm{RP}}) = \min F(V_s; T_S, P_{\mathrm{FA}}, \lambda_1, \lambda_2, \ldots, \lambda_S\}, \\
&f \leq R, \sum_{i=1}^{S} N_i = N.
\end{aligned} \tag{15}$$

To solve the last problem, [11] proposed two algorithms, namely the Hughes-Hartogs and discrete particle-swarm optimization (DPSO) algorithms. For a fixed SS frequency (f), the Hughes-Hartogs algorithm can find the optimal packet-loading results ($\{N_1, N_2, \ldots, N_S\}$); then, the DPSO algorithm is used to find the optimal particle in each iteration. After several iterations, we can obtain the optimal packet-loading results and SS frequency. The main problems of the two above-mentioned methods are their high complexity and large processing times, in particular DPSO. Actually, in CRSNs, there are many hardware restrictions, and practical nodes are usually embedded using only small CPUs and limited memories. Accordingly, the methods

Procedure 2.

1) *Firstly, Set* $f = f_{\min}$, $i = 1$, $i = Iteration\ Index$ *and Run Hughes–Hartogs algorithm* [5] *to calculate* $N^{(1)} = \{N_1, N_2, ..., N_S\}$ *then* $E^{(1)}(N_{\mathrm{RP}})$ *can be obtained from equation* (15).

2) *Increment the f value* : $f^{(i+1)} = f^{(i)} + 1$ *and update the iteration index* : $i = i + 1$

3) *If* $f \leq f_{\max}$ *then run Hughes – Hartogs algorithm again to calculate* $N^{(i)} = \{N_1, N_2, ..., N_S\}$ *and* $E^{(i)}(N_{RP})$ *then go to Step* 2 *Else if* $f > f_{\max}$ *then go to Step* 4.

4) *The optimal values of* N^* *and* f^* *can be achieved* directly based on minimun of $\{E^{(i)}(N_{\mathrm{RP}})$ for $\mathrm{i} = 1, 2, ..., f_{\max} - f_{\min}\}$ *from the equation* (16):

with lower processing times are preferred. As a result, we discard the high cost DPSO algorithm and propose our method, which uses the following procedure:

$$I = Arg(\min E^{(i)}(N_{\mathrm{RP}})), \quad i = 1, 2, \ldots . \tag{16}$$

By getting index "I" which minimizes $\{E^{(i)}(N_{\mathrm{RP}})$ for $i = 1, 2, \ldots, f_{\max} - f_{\min}\}$, it is easy to estimate $N^* = \{N_1^*, N_2^*, \ldots, N_S^*\}$ and f^* just by using following equations: $N^* = N^{(I)} = \{N_1^I, N_2^I, \ldots, N_S^I\}$ and $f^* = f^I$. Hence $(S + 1)$ variables $\{N_1^I, N_2^I, \ldots, N_S^I; f^I\}$ are estimated.

It should be noted that our numerical analysis of the $E(N_{\mathrm{RP}})$ functional behavior in terms of the f variation, especially the soft variations of f around f^*, shows that this function will experience a very smooth change around f^*. This important feature explicitly indicates that the high-accuracy estimation of f^* does not benefit the proposed transmission system. Moreover, its approximate calculation can reduce the total processing time. For example, applying the simple replacement of $f^{(i+1)} = f^{(i)} + 2$ instead of $f^{(i+1)} = f^{(i)} + 1$ (in Step 2 of our method) will reduce the overall processing time by 50%.

5. Image Scrambling and Filtering-Based PSNR Enhancement in Multichannel Communication (MC-SAFE)

In previous sections, we presented our enhanced methods for image transmission over CRSNs. The main parameter that is considered in the model is $D_{\max}$ or the maximum tolerable delay. However, in spite of our attempts to minimize the number of packets that remain in the send buffer, depending on the PUs' traffic, it is possible to have a timeout event without ending the image stream. In this case, the transmitter node prevents the transmission of the rest of the information of the input image. Consequently, on the other end of the channel, the receiver receives only a part of the image. This condition is depicted in Fig. 3. The input image is a 512 × 512 RGB image that includes three color channels: red, green, and blue. The black pixels in Fig. 3(f) are related to the packet loss. Actually, because of a timeout event, around 12% of all pixels remain in the send buffer. The sender node arranges the pixels from the first row of subchannel R to the last row of subchannel B as a vector (payload array) in the transmit buffer, after which it proceeds to send this vector. Chronologically, the last pixels of the B channel will be the last pixels that should be transmitted in the allowed time range: $[0, D_{\max}]$. In the case where a timeout event has occurred, the receiver fills the empty

Fig. 3. Black pixels show the lost packets due to a timeout event during transmission: (a) original (red), (b) original (green), (c) original (blue), (d) received (red), (e) received (green), and (f) received (blue).

rows and columns with zero values or equivalently black Pixels, which is called zero-padding.

In order to compare the performance of the image transmission system, we use the most important metrics to evaluate the image quality, that is, the PSNR. The PSNR definition is presented in (17) [2], [14]:

$$\begin{aligned} \mathrm{PSNR} &= 10\mathrm{Log}_{10}\frac{(2^n - 1)^2}{\mathrm{MSE}}, \\ \mathrm{MSE} &= \frac{\sum_{j=1}^{c}\sum_{i=1}^{r}\left|I_{\mathrm{Sender}} - I_{\mathrm{Receiver}}\right|^2}{r \times c}, \end{aligned} \tag{17}$$

where MSE is the mean square error. According to these formulations, the direct approach to improve the PSNR is to reduce the MSE between the transmitted and received images [14], [15]. In time-out situations, when there are black pixels with zero values in the last rows of the blue subimage, the MSE will increase. In addition, in this case, there is no way of enhancing the image quality based on typical image-processing methods, such as 3 × 3 average filters and smoothing filters (because such filters have no gain in the black parts related to the pixel loss; thus, no actual enhancement will be achieved).

To address this challenging issue, we propose the MC-SAFE method, which suggests the distribution of the black pixels throughout all of the three subimages instead of in just the last part of the blue image. In fact, to change the spatial position of the pixels, we first used a reversible scrambling function $g(x, y)$ to rearrange them in the RGB image I_{Sender} and generate a new image $\hat{I}$; then,

https://doi.org/10.4218/etrij.17.0116.0887

we converted three-two-dimensional (2D) matrices $\{\hat{I}_{\text{Red}}, \hat{I}_{\text{Green}}, \hat{I}_{\text{Blue}}\}$ into a vector V_{Sender} according to the following proposed procedure:

Procedure 3. Image Scrambling Befor Transmission

Get *Input* Image :

$$I_{\text{Sender}} = \{I_{\text{Red}}, I_{\text{Green}}, I_{\text{Blue}}\} \text{ with r} \times \text{c pixels}$$

Apply Transmission Function $T_{g(x,y)}$:

$$\hat{\text{I}} = T_{g(x,y)}\{I(x,y)\}$$

Split $\hat{\text{I}}$ *to* $\{\hat{I}_{\text{Red}}, \hat{I}_{\text{Green}}, \hat{I}_{\text{Blue}}\}$

Rearrangement *of* $\hat{\text{I}}$ *to make* V_{Sender} :

$$V_{\text{Sender}} = \{\left[\hat{I}_{\text{Red}}(\text{Row}_1), \hat{I}_{\text{Green}}, (\text{Row}_1), \hat{I}_{\text{Blue}}(\text{Row}_1)\right]...$$
$$.... \left[\hat{I}_{\text{Red}}(\text{Row}_2), \hat{I}_{\text{Green}}, (\text{Row}_2), \hat{I}_{\text{Blue}}(\text{Row}_2)\right] ..$$
$$.... \left[\hat{I}_{\text{Red}}(\text{Row}_r), \hat{I}_{\text{Green}}, (\text{Row}_r), \hat{I}_{\text{Blue}}(\text{Row}_r)\right]\}$$

The transmitter node sends V_{Sender} and the receiver will receive V^*_{Sender}. In a perfect transmission scenario, $V^*_{\text{Sender}} = V_{\text{Sender}}$, but in practice, owing to packet loss, some of the pixel positions in V^*_{Sender} may be empty. In this case, the empty pixel positions are then zero padded. Now, the receiver should reverse the procedure proposed for transmission by converting V^*_{Sender} to $(\hat{I})^*$, and then applying the inverse function $T^{-1}_{g(x,y)}\{(\hat{I})^*\}$ to obtain $I^{\text{Recounstructed}}_{\text{Receiver}}$. This is the best time to apply our image-processing enhancement method based on the 3 × 3 average filter to estimate the value of pixels using their eight neighbors located in the 3 × 3 mask around the central pixesl. The MC-SAFE approach not only can markedly enhance the PSNR of the image, but also it can improve the maximum tolerable delay effectively. This improvement will be discussed in more detail in the next section.

III. Simulation and Results

As previously presented, our work focuses on image transmission over CRSNs. In order to investigate the performance of our proposed algorithm, we used "lena.bmp," which is an eight-bit RGB image with a size 512 × 512. We take advantage of the main performance metric in image transmission, that is, the PSNR, to evaluate the performance of the algorithm in different conditions.

In our model, we defined N and f as optimizing parameters to minimize our cost function $E(N_{\text{RP}})$. According to (4) and (13), important parameters such as $\{\lambda_i, T_{\text{S}}, P_{\text{fa}}, N, R_i, S, D_{\max}\}$ can affect this nonlinear function; thus, we considered these parameters in our simulations using Matlab software, and we investigated appropriate values based on related literatures [2], [11], [16]. Table 1 shows these parameters along with their descriptions.

Table 1. Parameters defined in the model.

Row	Parameter	Description
1	N	Number of packets in input image
2	R_i	Channel capacity
3	f_i	Spectrum sensing frequency
4	λ_i	Arrival rate of pus
5	T_{s}	Spectrum sensing duration time
6	$D_{\max}$	Maximum tolerable delay
7	S	Number of available channels in pool
8	P_{fa}	Probability of false alarm

First, we evaluate the proposed DPUP and its impact on the system functionality. We consider the situation:

$R_i = 800, N = 650, D_{\max} = 1.1\,\text{s}, S = 10, P_{\text{fa}} = 0.02, T_{\text{s}} = 0.02$, and we assume that the PUs' traffic is sufficient low to enable the continuous transmission of all of the input image Lena on just one channel. By applying the proposed dynamic procedure that was previously mentioned, both $D_{\max}{}^{(K+1)}$ *and* $N^{(K+1)}$ are updated to provide a dynamic estimation of $f_i^{(K+1)}$ for each SS iteration (SSI) K. In Fig. 4, the optimal frequency f^* is estimated to be around 89 at the beginning phase of the transmission for the first SSI (SSI = 1); then, it falls sharply to 29 for SSI = 2. Next, f^* shows a soft decline trend down to 10 from SSI = 3 to SSI = 29. Finally, the new value is raised up to 25 for SSI = 41 at the end point of transmission. This "U" shaped variation in the f^* pattern is well adapted to time-variant channel scenarios. To elaborate, in the initial phase, our proposed algorithm tries to send as many packets as possible, around 89, for SSI = 1. The SU's arrival time is the random time point between two successive PU intervals, and will take $\mu_i = (\lambda_i)^{-1}$ seconds on average. If this time point is near the left side of the idle time window, the selection of a higher f^* will be the best action, as performed by our algorithm. On the other hand, if it is far from the left side,

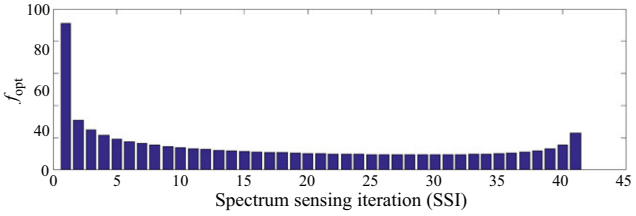

Fig. 4. Variation of optimal frequency based on dynamic updating of parameters.

this implicitly means that we have a few *channels available time*; therefore, the HO (and consequently retransmission) will be unavoidable in the next SS for both low and high values of f*. As a result, a larger value may be a better choice provided that the SU arrival time is sufficient to ensure no collision for the first SS.

After SSI = 1, if the channel is still available, our algorithm will update the parameters and try to reduce the f* gradually from 29 to 10 in order to decrease the collision probability. For SSI = 29, about 25% of the total packets are still in the transmitting queue; thus, f* should be increased to complete the transmission within the short remaining time. At the final attempt, for SSI = 41, the nodes empty the buffers by sending all of the remaining packets.

Now, we analyze the behavior of our proposed methods in terms of channel decision and ranking. We set the parameters to the following values: $R_i = 700, N = 650$, $D_{\max} = 1\,\text{s}, S = 10$, $P_{\text{fa}} = 0.01, T_{\text{s}} = 0.01$, and we then apply three different scenarios:

$$\lambda^{(1)} = [300\ 600\ 900\ 1200\ 1500\ 1800\ 2100\ 2400\ 2700\ 3000],$$
$$\lambda^{(2)} = [3000\ 2700\ 2400\ 2100\ 1800\ 1500\ 1200\ 900\ 600\ 300],$$
$$\lambda^{(3)} = [300\ 300\ 300\ 300\ 300\ 300\ 300\ 300\ 300\ 300].$$

In scenario (1), the arrival rates of the PU's channel increase from 300 (arrivals per second) in channel 1 to 3,000 in channel 10. In this case, channels 1 and 10 are clearly the best and worse channels, respectively (from the CR user perspective). Figure 5 shows the channel's histogram for transmission of ''Lena.bmp.'' In this figure, the vertical and horizontal axes represent the number of iterations of each channel in the image-transmission process and the channel index, respectively. The results of Fig. 5(b) clearly show that our proposed method effectively selects the best channel (channel 1 with 14 iterations), the second best channel (channel 2 with 12 iterations), and the third best channel (channel 3 with 6 iterations). Our channel decision and ranking algorithm avoids channels with high arrival rates to reduce the probability of collisions in the system. Conversely, in scenario (2), the arrival rates for channels 1 to 10 vary from 3,000 to 300. The results show the same rule indicated in scenario (1) for channels 10, 9, and 8. Here, the worse channels, such as 1, 2, and 3, have no share in data transmission in the systems (Fig. 5(c)). In the last scenario, we assume that all channels have the same value of arrival rate, that is, about 300. In this case, our method tries to select all 10 available channels, and balances the transmission load in the spectrum band (please refer to Fig. 5(a)). The results of these three scenarios verify that our proposed method rigidly tries to involve just the channels that have the appropriate conditions in order to reduce the probability of retransmission (because retransmission has a high cost on the actual time of transmission). Actually, providing that there is a retransmission, the probability of successful transmission of an image within the time range [0, Dmax] will decrease.

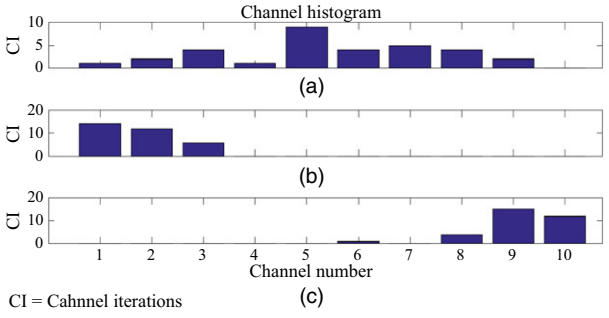

Fig. 5. Channel histograms for different PU arrival rates: (a) equal rate, (b) incremental rate, and (c) deceremental rate.

In addition, we performed our evaluation of the proposed method by setting the model parameters as follows:

$$R_i = 700, N = 550, D_{\max} = 1.5\text{s}, S = 10,\ P_{\text{fa}} = 0.01, T_{\text{s}} = 0.01,$$
$$\lambda = [20\ 40\ 60\ 80\ 100\ 120\ 140\ 160\ 180\ 200].$$

Figure 6 shows the original color image (Lena) at the sender with three sub images in R, G, and B channels. The results of our model when transmitting an image over CRSNs are depicted in Figs. 6(e), (f), (g), and (h). In order to compare the subchannel degradation, the error energy of each channel is calculated separately, and the outcomes strongly indicate that in this case, there is a zero energy error for all color channels at the receiver sensor node. This is confirmed by Figs. 6(i), (j), (k), and (l), for the final RGB color in the receiver sensor node. The results of Fig. 6 show that in this example, we do not have any loss; thus, we obtain PSNR = Inf.

To continue our analysis, we present Fig. 7. Figure 7(a) shows the value of "f" in terms of the SSI, while Fig. 7(b) shows the channel number indicator (CNI). From the figure, the total numbers of SS and HO iterations are 24 and 8 respectively. As a consequence, our algorithm tries to assign a lower f when an HO event forces the sensor node to switch to the channel with a higher arrival rate. For example, after SSI = 3, the transmitter node performs an HO from CNI = 1 (with λ_1 = 200) to CNI = 2 (with λ_2 = 400), and owing to this change, f decreases from 24

https://doi.org/10.4218/etrij.17.0116.0887

Fig. 6. Error Energy Comparison: original image with its channels at the transmitter node (a) red, (b) green, (c) blue, (d) color, received with its sub channels at the received node (e) red, (f) green, (g) blue, (h) color, and error Energy Images for all images (i) red, (j) green, (k) blue, (l) color.

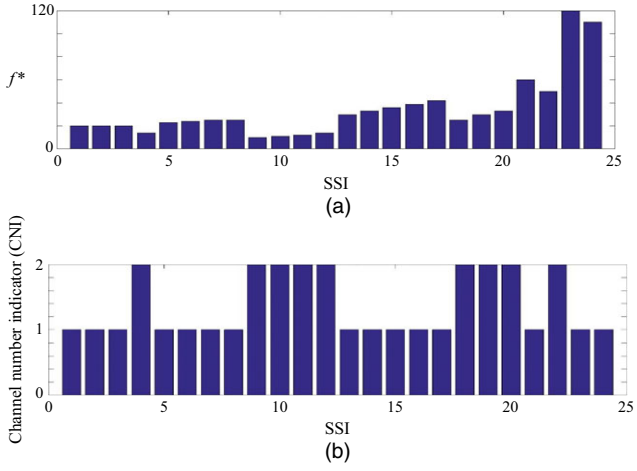

Fig. 7. f and CNI vs SSI: (a) estimated values of f^* during transmission and (b) channel number status during transmission.

to 16. This behavior of our algorithm intelligently reduces the probability of collision in the higher arrival rate channel, and consequently, the number of retransmissions will be decreased by only the dynamic adaptation of "f" to the channels' new conditions. Consider the case where SSI = 12. Then, a new arrival is detected, and consequently, an HO is performed from CNI = 2 to CNI = 1. In the new channel, our algorithm doubles f to 31 in order to decrease the SS time overhead in the lower arrival rate channel (CNI = 1). In addition, from SSN = 13 to SNN = 17, there is no need for any HOs; the value of "f" is increased adaptively from 31 to 43 by our algorithm in order to further empty the transmission buffer.

We applied a tight restriction to the previous scenarios by keeping constant all of the parameters except $D_{\max}$. It is redefined to decrease from 1.0 s to 0.75 s in the new simulation. The new results are shown in Figs. 8(a), (b), (c), and (d). Here, the transmitter sensor node runs fifteen SS iterations during transmission and accordingly, there are five HOs. The error energy image in Fig. 8(d) indicates that the received image has degraded owing to packet loss. In this situation, 11.09% of the transmitted data are lost, and we achieve PSNR = 20.36 (Fig. 9(a) and (b)).

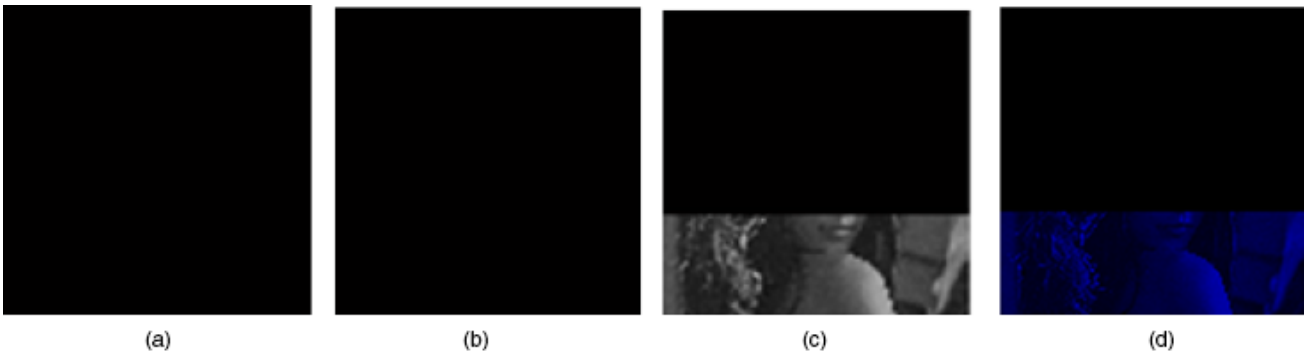

Fig. 8. Error energy after the tim eout event occurrence: (a) red, (b) green, (c) blue, and (d) received.

Fig. 9. (a) Original and (b) received images after timeout event.

Ultimately, we want to investigate the image-based PSNR enhancement method that has been proposed in the previous section. With this approach, the sending vector (V_{Sender}) is generated, and will be transmitted through the channel. By applying a reversible mapping function $g(x, y)$, and rearranging all the pixels in the RGB image in the sender node, the remaining pixels that emerge as black pixels in the reconstructed image (at the receiver) will be distributed randomly throughout the image (not only in the blue subchannel). This effect is well depicted in Figs. 10(a), (b), and (c), and their error energy images are shown in Figs. 10(d), (e), and (f). The obtained image $I^{\text{Receiver}}_{\text{Reconstructed}}$ can be filtered by applying our 3×3 average filter to get an enhanced image I^{*}_{Sender}. Both I^{*}_{Sender} and its error energy are presented in Figs. 11(b), and (c). The results indicate that there is a PSNR enhancement of around 5 dB compared with the conventional approach without scrambling and filtering. Finally, in Table 2, we compare our methods with other approaches for these conditions:

$$S = 4, \lambda_i = [5 - 9], D_{\max} = [0.35,\ 40,\ 0.45, 1, 195].$$

The obtained results clearly indicate that our approaches, in particular MCPL-SAFE, are much more beneficial with respect to PSNR compared to the other mentioned algorithms. It should be noted that according to this table, when $D_{\max}$ is sufficient to achieve perfect transmission with PSNR = Inf, the result of the proposed filtering-based method, MCPL-SAFE, is degraded compared with other algorithms without filtering. This is due to the direct effect of the smoothing filter, which replaces the true value of each pixel by the average of its eight neighbors' pixel values. This replacement consequently increases the MSE and decreases the PSNR.

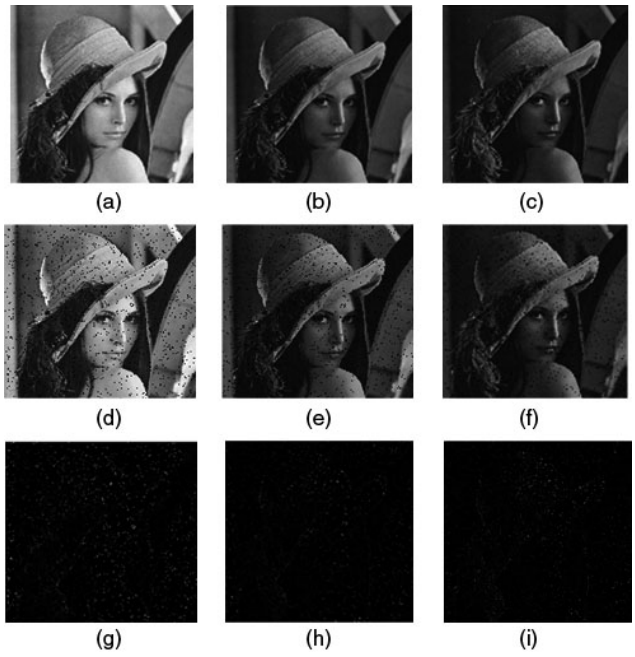

Fig. 10. Distributing the black pixels to all sub channels by scrambling and rearrangement of all pixels: (a) original (red), (b) original (green), (c) original (blue), (d) received (red), (e) received (green), (f) received (blue), (g) error energy (red), (h) error energy (green), and (i) error energy (blue).

https://doi.org/10.4218/etrij.17.0116.0887

Fig. 11. Original and enhanced received images comparison after the timeout event occurrence (MC-SAFE): (a) original, (b) received (enhanced), and (c) error energy (enhanced).

Table 2. Comparison results.

PSNR (in dB)					
D_{max}	Huang [11]	Equal packet-loading [11], [16]	Da Silva [17]	Proposed	
				MCPL	MCPL-SAFE
0.35 s	16.80	16.76	7.39	17.11	24.85
0.40 s	18.99	17.84	7.39	19.24	26.61
0.45 s	19.01	18.02	7.39	19.35	27.70
1.05 s	25.49	24.72	7.41	26.85	31.25
195 s	Inf	Inf	17.1	Inf	32.63

IV. Conclusion

In traditional WSNs, the bandwidth constraint due to public standards, such as IEEE 802.15.4, is a major obstacle to achieving high QoS multimedia transmission. Therefore, we conducted our research using more efficient approaches based on CRSNs. In this paper, we introduced our enhanced model for image transmission over CRSNs. The results obtained show that our algorithm significantly enhances the PSNR in the receiver node.

References

[1] R. Mohammadi and A. Ghaffari, "Optimizing Reliability Through Network Coding in Wireless Multimedia Sensor Networks," *Indian J. Sci. Technol.*, vol. 8, no. 9, May 2015, pp. 834–841.

[2] M. Bahaghighat and S.A. Motamedi, "IT-MAC: Enhanced MAC Layer for Image Transmission Over Cognitive Radio Sensor Networks," *Int. J. Comput. Sci. Inform. Security*, vol. 14, no. 12, Dec. 2016, pp. 234–241.

[3] N.M. Aripin et al., "Cross Layer Design of Multimedia Transmission Over Cognitive Radio UWB Multiband OFDM System," *Proc. Int. Graduate Conf. Eng. Sci.*, Dec. 23–24, 2008.

[4] O.B. Akan, O.B. Karli, and O. Ergul, "Cognitive Radio Sensor Networks," *IEEE Netw.*, vol. 23, no. 4, July-Aug. 2009, pp. 34–40.

[5] A.O. Bicen, V.C. Gungor, and O.B. Akan, "Delay-Sensitive and Multimedia Communication in Cognitive Radio Sensor Networks," *Ad Hoc Netw.*, vol. 10, no. 5, July 2012, pp. 816–830.

[6] H. Wang, Y. Qian, and H. Sharif, "Multimedia Communications Over Cognitive Radio Networks for Smart Grid Applications," *IEEE Wireless Commun.*, vol. 20, no. 4, Aug. 2013, pp. 125–132.

[7] W.-Y. Lee and I.F. Akyildiz, "Optimal Spectrum Sensing Framework for Cognitive Radio Networks," *IEEE Trans. Wireless Commun.*, vol. 7, no. 10, Oct. 2008, pp. 3845–3857.

[8] A. Homayounzadeh and M. Mahdavi, "Improving Voice-Service Support in Cognitive Radio Networks," *ETRI J.*, vol. 38, no. 3, June 2016, pp. 444–454.

[9] J. Zuo et al., "Energy-Efficiency Power Allocation for Cognitive Radio MIMO-OFDM Systems," *ETRI J.*, vol. 36, no. 4, Aug. 2014, pp. 686–689.

[10] N.-M. Kim et al., "Robust Cognitive-Radio-Based OFDM Architecture with Adaptive Traffic Allocation in Time and Frequency," *ETRI J.*, vol. 30, no. 1, Feb. 2008, pp. 21–32.

[11] X.-L. Huang et al., "The Impact of Spectrum Sensing Frequency and Packet-Loading Scheme on Multimedia Transmission Over Cognitive Radio Networks," *IEEE Trans. Multimedia*, vol. 13, no. 4, Aug. 2011, pp. 748–761.

[12] G.A. Shah and O.B. Akan, "Performance Analysis of CSMA-Based Opportunistic Medium Access Protocol in Cognitive Radio Sensor Networks," *Ad Hoc Netw.*, vol. 15, 2014, pp. 4–13.

[13] Z. Liang, S. Feng, and D. Zhao, "Supporting Random Real-Time Traffic in a Cognitive Radio Sensor Network," *Veh. Technol. Conf. Fall*, Ottawa, Canada, Sept. 6–9, 2010, pp. 1–5.

[14] Z. He and S. Mao, "Adaptive Multiple Description Coding and Transmission of Uncompressed Video Over 60GHz Networks," *ACM SIGMOBILE Mobile Comput. Commun. Rev.*, vol. 18, no. 1, Jan. 2014, pp. 14–24.

[15] M. Manohara et al., "Error Correction Scheme for Uncompressed HD Video Over Wireless," *IEEE Int. Conf. Multimedia Expo*, New York, USA, June 28–July 3 2009, pp. 802–805.

[16] H. Kushwaha et al., "Reliable Multimedia Transmission Over Cognitive Radio Networks Using Fountain Codes," *Proc. IEEE*, vol. 96, no. 1, Jan. 2008, pp. 155–165.

[17] C.A. da Silva et al., "Towards WMSN Performance Using Different Packet Size," *IEEE SENSORS*, Orlando, FL, USA, Oct. 30–Nov. 3, 2016, pp. 1–3.

Mahdi Bahaghighat received the M.Sc. degree in Telecommunication Systems from the Iran University of Science and Technology (IUST), Tehran, Iran, in 2007. He joined the Department of Electrical and Computer Engineering, Raja University of Qazvin, as a Lecturer, at 2008. In 2012, he became a PhD student at Amirkabir University of Technology (AUT), Tehran. His current research interests include Wireless Sensor and Ad-hoc Networks, Cognitive Radio, Wireless Multimedia Transmission, Image Processing and Computer Vision.

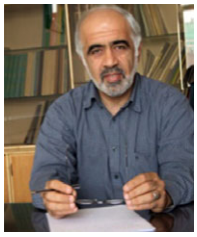

Seyed Ahmad Motamedi got his BS in Electronic Engineering from Amirkabir University of Technology (AUT), Tehran, Iran, in 1978, and his MS and PhD, both in Digital Electronics and Informatics Systems, from Pierre and Marie Curie University, France, in 1980 and 1983, respectively. He has been a faculty member of the Electrical Engineering Department of AUT since 1984, where he has also been the chancellor since June 2014. His current research interests include Digital Electronics, Parallel Processing, Image Processing, Wireless Sensor Networks, and Cloud Computing.

https://doi.org/10.4218/etrij.17.0116.0887